PHYSICAL REVIEW D **75,** 111101(R) (2007)

Search for $B^0 \to p\bar{p}$, $\Lambda\bar{\Lambda}$ and $B^+ \to p\bar{\Lambda}$ at Belle

Y.-T. Tsai,[23] P. Chang,[23] K. Abe,[7] I. Adachi,[7] H. Aihara,[39] D. Anipko,[1] A. M. Bakich,[35] U. Bitenc,[11] I. Bizjak,[11] S. Blyth,[21] M. Bračko,[7,17,11] T. E. Browder,[6] M.-C. Chang,[4] Y. Chao,[23] A. Chen,[21] W. T. Chen,[21] B. G. Cheon,[5] R. Chistov,[10] Y. Choi,[34] S. Cole,[35] J. Dalseno,[18] M. Danilov,[10] M. Dash,[43] J. Dragic,[7] A. Drutskoy,[3] S. Eidelman,[1] S. Fratina,[11] N. Gabyshev,[1] H. Ha,[13] J. Haba,[7] H. Hayashii,[20] M. Hazumi,[7] D. Heffernan,[28] Y. Hoshi,[37] W.-S. Hou,[23] Y. B. Hsiung,[23] T. Iijima,[19] K. Ikado,[19] K. Inami,[19] A. Ishikawa,[39] R. Itoh,[7] M. Iwasaki,[39] Y. Iwasaki,[7] J. H. Kang,[44] H. Kawai,[2] H. Kichimi,[7] H. J. Kim,[14] H. O. Kim,[34] K. Kinoshita,[3] S. Korpar,[17,11] P. Križan,[16,11] P. Krokovny,[7] R. Kulasiri,[3] R. Kumar,[29] C. C. Kuo,[21] A. Kuzmin,[1] Y.-J. Kwon,[44] M. J. Lee,[32] Y.-J. Lee,[23] T. Lesiak,[24] A. Limosani,[7] S.-W. Lin,[23] D. Liventsev,[10] T. Matsumoto,[41] S. McOnie,[35] T. Medvedeva,[10] W. Mitaroff,[8] H. Miyata,[26] Y. Miyazaki,[19] G. R. Moloney,[18] E. Nakano,[27] M. Nakao,[7] Z. Natkaniec,[24] S. Nishida,[7] O. Nitoh,[42] S. Ogawa,[36] T. Ohshima,[19] S. Okuno,[12] Y. Onuki,[31] H. Ozaki,[7] P. Pakhlov,[10] G. Pakhlova,[10] L. E. Piilonen,[43] Y. Sakai,[7] N. Satoyama,[33] T. Schietinger,[15] O. Schneider,[15] J. Schümann,[7] K. Senyo,[19] M. E. Sevior,[18] M. Shapkin,[9] H. Shibuya,[36] J. B. Singh,[29] A. Somov,[3] M. Starič,[11] H. Stoeck,[35] T. Sumiyoshi,[41] F. Takasaki,[7] M. Tanaka,[7] G. N. Taylor,[18] Y. Teramoto,[27] X. C. Tian,[30] I. Tikhomirov,[10] S. Uehara,[7] K. Ueno,[23] Y. Unno,[5] S. Uno,[7] P. Urquijo,[18] G. Varner,[6] K. E. Varvell,[35] S. Villa,[15] A. Vinokurova,[1] C. H. Wang,[22] M.-Z. Wang,[23] Y. Watanabe,[40] E. Won,[13] A. Yamaguchi,[38] Y. Yamashita,[25] M. Yamauchi,[7] V. Zhilich,[1] V. Zhulanov,[1] and A. Zupanc[11]

(The Belle Collaboration)

[1]*Budker Institute of Nuclear Physics, Novosibirsk*
[2]*Chiba University, Chiba*
[3]*University of Cincinnati, Cincinnati, Ohio 45221*
[4]*Department of Physics, Fu Jen Catholic University, Taipei*
[5]*Hanyang University, Seoul*
[6]*University of Hawaii, Honolulu, Hawaii 96822*
[7]*High Energy Accelerator Research Organization (KEK), Tsukuba*
[8]*Institute of High Energy Physics, Vienna*
[9]*Institute of High Energy Physics, Protvino*
[10]*Institute for Theoretical and Experimental Physics, Moscow*
[11]*J. Stefan Institute, Ljubljana*
[12]*Kanagawa University, Yokohama*
[13]*Korea University, Seoul*
[14]*Kyungpook National University, Taegu*
[15]*Swiss Federal Institute of Technology of Lausanne, EPFL, Lausanne*
[16]*University of Ljubljana, Ljubljana*
[17]*University of Maribor, Maribor*
[18]*University of Melbourne, School of Physics, Victoria 3010*
[19]*Nagoya University, Nagoya*
[20]*Nara Women's University, Nara*
[21]*National Central University, Chung-li*
[22]*National United University, Miao Li*
[23]*Department of Physics, National Taiwan University, Taipei*
[24]*H. Niewodniczanski Institute of Nuclear Physics, Krakow*
[25]*Nippon Dental University, Niigata*
[26]*Niigata University, Niigata*
[27]*Osaka City University, Osaka*
[28]*Osaka University, Osaka*
[29]*Panjab University, Chandigarh*
[30]*Peking University, Beijing*
[31]*RIKEN BNL Research Center, Upton, New York 11973*
[32]*Seoul National University, Seoul*
[33]*Shinshu University, Nagano*
[34]*Sungkyunkwan University, Suwon*
[35]*University of Sydney, Sydney, New South Wales*
[36]*Toho University, Funabashi*
[37]*Tohoku Gakuin University, Tagajo*

[38]*Tohoku University, Sendai*
[39]*Department of Physics, University of Tokyo, Tokyo*
[40]*Tokyo Institute of Technology, Tokyo*
[41]*Tokyo Metropolitan University, Tokyo*
[42]*Tokyo University of Agriculture and Technology, Tokyo*
[43]*Virginia Polytechnic Institute and State University, Blacksburg, Virginia 24061*
[44]*Yonsei University, Seoul*
(Received 30 March 2007; published 15 June 2007)

We report on a new search for two-body baryonic decays of the B meson. Improved sensitivity compared to previous Belle results is obtained from 414 fb^{-1} of data that corresponds to 449×10^6 $B\bar{B}$ pairs, which were taken on the $\Upsilon(4S)$ resonance and collected with the Belle detector at the KEKB e^+e^- collider. No significant signals are observed and we set the 90% confidence level upper limits: $\mathcal{B}(B^0 \to p\bar{p}) < 1.1 \times 10^{-7}$, $\mathcal{B}(B^0 \to \Lambda\bar{\Lambda}) < 3.2 \times 10^{-7}$, and $\mathcal{B}(B^+ \to p\bar{\Lambda}) < 3.2 \times 10^{-7}$.

DOI: 10.1103/PhysRevD.75.111101 PACS numbers: 13.25.Hw

Recent observations of B meson decays into several charmless three-body baryonic final states show branching fractions around 10^{-6} and a peak in the baryon-antibaryon mass spectra near threshold [1]. Further investigations of the angular correlations for events in the threshold region [2] favor a fragmentation model [3]. In contrast, charmless two-body baryonic B decays are expected to have lower branching fractions. However, it is challenging to perform conclusive theoretical calculations of baryon formation in B decay. Previous searches [4,5] for two-body decays yielded upper limits on the branching fractions of $(3-7) \times 10^{-7}$, which are consistent with a recent calculation using the pole model [6] but in contradiction with a calculation based on QCD sum rules [7]. Moreover, the upper limit for $B^0 \to p\bar{p}$ is also consistent with simple scaling of the measured branching fraction for $B^0 \to \Lambda_c^- p$ [8] by the current estimate of $|V_{ub}/V_{cb}|^2$, which gives $\mathcal{B}(B^0 \to p\bar{p}) \sim 2.0 \times 10^{-7}$.

Two-body baryonic decays provide valuable guidance to improve the understanding of quark/gluon fragmentation of the B meson to baryons. In this article we report searches with better sensitivity for the charmless two-body baryonic B decays $B^0 \to p\bar{p}$, $B^0 \to \Lambda\bar{\Lambda}$, and $B^+ \to p\bar{\Lambda}$ [9]. The analysis is based on a 414 fb^{-1} data sample, corresponding to 449×10^6 $B\bar{B}$ pairs, accumulated at the $\Upsilon(4S)$ resonance with the Belle detector at the KEKB [10] asymmetric e^+e^- collider.

The Belle detector is a large-solid-angle magnetic spectrometer that consists of a silicon vertex detector (SVD), a 50-layer central drift chamber (CDC), an array of aerogel threshold Cherenkov counters (ACC), time-of-flight scintillation counters (TOF), and an array of CsI(Tl) crystals, all located inside a superconducting solenoid coil that provides a 1.5 T magnetic field. An iron flux-return located outside of the coil is instrumented to detect K_L^0 mesons and to identify muons. The detector is described in detail elsewhere [11]. Two different inner detector configurations were used. For the first sample of 152×10^6 $B\bar{B}$ pairs, a 2.0 cm radius beampipe and a 3-layer silicon vertex detector (SVD1) were used; for the latter 297×10^6 $B\bar{B}$ pairs, a 1.5 cm radius beampipe, a 4-layer silicon detector (SVD2) [12], and a small-cell inner drift chamber were used.

Primary charged tracks associated with candidate B decays are required to satisfy the following criteria: the track impact parameters relative to the run-by-run interaction point (IP) are required to be within ± 2 cm along the z axis (oriented antiparallel to the positron beam) and within ± 0.05 cm in the transverse (xy) plane.

Proton candidates are selected based on the likelihood functions L_p, L_K, and L_π for protons, kaons, and pions, respectively, which are determined from particle identification information from the CDC (dE/dx specific ionization), the ACC (Cherenkov radiation pulse height), and the TOF (time relative to the beam bunch crossing). Charged tracks with $L_p/(L_p + L_\pi) > 0.6$ are identified as protons and $L_\pi/(L_p + L_\pi) > 0.6$ as pions. For proton candidates that originate directly from B decays, an additional requirement, $L_p/(L_p + L_K) > 0.6$, is applied to improve the purity. The proton identification efficiency with the tighter requirements is 77% for 2 GeV/c protons.

Λ candidates are reconstructed from oppositely charged pion-proton pairs, satisfying the following criteria: the separation distance between the pion and proton at the Λ decay vertex must be less than 12.9 cm along the z axis; the distance of the closest approach in the xy plane to the IP is greater than 0.008 cm for each track; the flight length of the Λ candidates must be greater than 0.22 cm in the xy plane; the angular difference between the Λ momentum vector and the vector between the IP and the Λ decay vertex must be less than 0.09 rad. Finally, the reconstructed invariant mass of Λ candidate is required to be within the mass interval (1.116 ± 0.005) GeV/c^2, corresponding to $\pm 3\sigma$ in the mass resolution.

B candidates are reconstructed by pairing two baryons and are identified with two kinematic variables: the beam-energy constrained mass, $M_{\text{bc}} = \sqrt{E_{\text{beam}}^2/c^4 - p_B^2/c^2}$, and the energy difference, $\Delta E = E_B - E_{\text{beam}}$, where E_{beam} is the run-dependent beam energy in the center-of-mass (c.m.) frame and p_B and E_B are reconstructed momentum and energy of the reconstructed B candidates in the c.m. frame, respectively. The signal region is defined as $5.27\ \mathrm{GeV}/c^2 < M_{\rm bc} < 5.29\ \mathrm{GeV}/c^2$ and $|\Delta E| < 0.05$ GeV, while the sideband region is defined as $5.2\ \mathrm{GeV}/c^2 < M_{\rm bc} < 5.26\ \mathrm{GeV}/c^2$ and $|\Delta E| < 0.2$ GeV.

All possible backgrounds are investigated using a GEANT3 [13] based Monte Carlo (MC) simulation. Backgrounds from the charmful and charmless B decays are found to be negligible. The dominant background is from continuum $e^+e^- \to q\bar{q}(q = u, d, s, c)$ events, which are studied using the sideband data.

Continuum background is suppressed by requiring $|\cos\theta_{\rm th}| < 0.9$, where $\theta_{\rm th}$ is the angle in the c.m. frame between the direction of one B daughter and the thrust axis [14], formed by the particles not associated with the B candidate. The $\cos\theta_{\rm th}$ distribution is nearly flat for signal but strongly peaks at ± 1 for the continuum.

The background rejection is further improved using event topology, B candidate vertex, and B flavor tagging information. First, we combine a set of modified Fox-Wolfram moments [15] into a Fisher discriminant [16] $\mathcal{F}$ to distinguish spherically distributed $B\bar{B}$ events from the jetlike continuum backgrounds. Figure 1(a) shows the Fisher discriminant for $p\bar{p}$ signal MC and sideband events. We then use the cosine of the angle θ_B between the B candidate flight direction and the z axis [Fig. 1(b)]. For the $p\bar{p}$ mode only, we use the distance Δz along the z axis between the $p\bar{p}$ vertex and the vertex formed from the remaining charged tracks [Fig. 1(c)]. The Δz probability density function is modeled by a double Gaussian independently for the SVD1 and SVD2 data due to the better vertex resolution provided by the SVD2. The PDFs for $\cos\theta_B$ and $\mathcal{F}$ are described by a second order polynomial and a double asymmetric Gaussian, respectively. The quantities $\mathcal{F}$, $\cos\theta_B$, and Δz (for the $p\bar{p}$ mode only) are combined to form likelihoods $\mathcal{L}_S$ and $\mathcal{L}_B$ for signal and continuum background, respectively. The normalized ratio $\mathcal{R} = \mathcal{L}_S/(\mathcal{L}_S + \mathcal{L}_B)$, shown in Fig. 1(d), peaks at unity for signal and at zero for continuum.

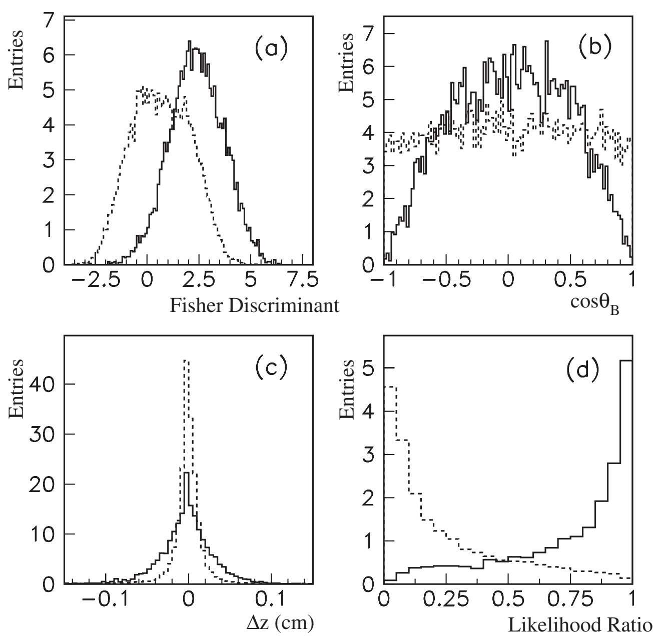

FIG. 1. Distributions of (a) the Fisher discriminant, (b) $\cos\theta_B$, (c) Δz, and (d) likelihood ratio for $B^0 \to p\bar{p}$ candidates. The solid histogram is for signal MC, while the dashed histogram is for sideband events.

The distribution of $\mathcal{R}$ is somewhat correlated with the event's B flavor information. The standard Belle flavor tagging algorithm [17] provides a tagging quality factor r that ranges from zero for no flavor tagging information to unity for unambiguous flavor assignment. We apply a requirement on the likelihood ratio $\mathcal{R}$ depending on the value of r (and on the inner detector configuration for the $p\bar{p}$ mode). The likelihood ratio requirements listed in Table I are determined by optimizing the figure-of-merit, $N_S/\sqrt{N_S + N_B}$, where N_S and N_B are the expected signal and background yields. The signal yields are estimated from the product of the number of $B\bar{B}$ events, the signal efficiency from MC and the assumed branching fraction of 10^{-7}. The expected background yields are obtained by scaling the amount of data in the region, $|\Delta E| < 0.05$ GeV and $5.2\ \mathrm{GeV}/c^2 < M_{\rm bc} < 5.26\ \mathrm{GeV}/c^2$, to the signal region. The $M_{\rm bc}$ distribution of the continuum is assumed to be independent of ΔE. Therefore, we model the $M_{\rm bc}$ distribution with an ARGUS function [18] using the data in $0.1\ \mathrm{GeV} < |\Delta E| < 0.2$ GeV. The scaling factor is estimated to be the ratio of the area of the $M_{\rm bc}$ signal region to the sideband region based on the ARGUS function.

The B signal efficiency for each mode is obtained using the MC simulation after applying all analysis requirements except the proton identification. The B signal efficiency is corrected for the proton identification; the proton identification efficiency is estimated using $\Lambda \to p\pi^-$ decays in data. The systematic error in the B signal efficiency arises from proton identification, tracking efficiency, Λ selection and the likelihood ratio requirement in each flavor-tagged region. The statistical error in the proton efficiency obtained in the Λ sample is included in the systematic error for proton identification. The tracking systematic error is studied using an inclusive $D^{*+} \to D^0\pi^+$ sample, where $D^0 \to K_S^0\pi^+\pi^-$ and $K_S^0 \to \pi^+\pi^-$. Candidate D^{*+} mesons are kinematically identified using the momentum of the

TABLE I. Minimum values of the likelihood ratio $\mathcal{R}$ for three ranges of the flavor tagging quality r (and for the inner detector configuration for the $p\bar{p}$ mode).

	$0 \le r < 0.5$		$0.5 \le r \le 0.75$		$0.75 < r \le 1.0$	
	SVD1	SVD2	SVD1	SVD2	SVD1	SVD2
$B^0 \to p\bar{p}$	0.85	0.85	0.8	0.65	0.65	0.65
$B^0 \to \Lambda\bar{\Lambda}$	0.85		0.6		0.35	
$B^+ \to p\bar{\Lambda}$	0.8		0.75		0.65	

TABLE II. Summary of systematic errors, given in percent.

	$B^0 \to p\bar{p}$	$B^0 \to \Lambda\bar{\Lambda}$	$B^+ \to p\bar{\Lambda}$
Tracking	2.00	4.29	3.16
PID	0.40	0.12	0.26
$\mathcal{R}$ Requirement	3.70	1.22	0.75
Λ Selection	-	4.50×2	4.50
$\mathcal{B}(\Lambda \to p\pi^-)$	-	1.56	0.78
# of $B\bar{B}$	1.27	1.27	1.27
Total (%)	4.42	10.24	5.76

slow pion from the D^{*+} decay, D^0 and K_S^0 mass constraints, and the trajectory of one of the pions in the K_S^0 decay. The tracking efficiency is measured by searching for the other K_S^0 daughter; by comparing the efficiency in data with the Monte Carlo expectation, the tracking systematic error is found to be 1% per track for $p > 0.3$ GeV/c but slightly larger for low momentum particles. The systematic error associated with requiring a detached vertex for the Λ candidate is studied by comparing the ratio of $D^+ \to K_S^0\pi^+$ and $D^+ \to K^-\pi^+\pi^+$ yields with the MC expectation. The resulting K_S^0 detection systematic error is $\pm 4.5\%$, which is used as the Λ systematic error. The likelihood ratio requirement is studied using control samples with the same number of charged particles in the final state: $B^0 \to K^+\pi^-$ for $p\bar{p}$, $B^0 \to D^-\pi^+ \to (K^+\pi^-\pi^-)\pi^+$ for $\Lambda\bar{\Lambda}$, and $B^+ \to \bar{D}^0\pi^+ \to (K^+\pi^-)\pi^+$ for $p\bar{\Lambda}$. The total systematic uncertainty is computed by adding the correlated errors linearly, and then adding the uncorrelated ones in quadrature. The systematic errors are summarized in Table II.

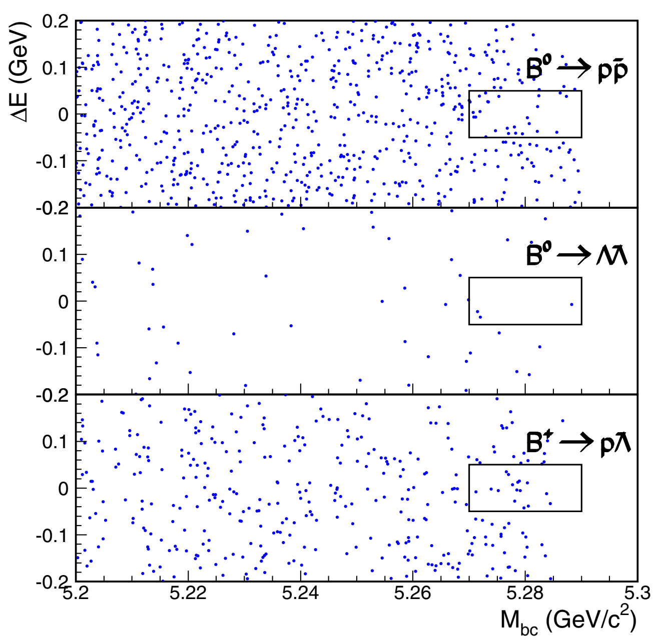

2 FIG. 2 (color online). Scatter plots of ΔE vs M_{bc} for $B^0 \to p\bar{p}$ (upper), $B^0 \to \Lambda\bar{\Lambda}$ (middle), and $B^+ \to p\bar{\Lambda}$ (lower). The signal region is indicated by the rectangle in each plot.

TABLE III. Summary of the $B^0 \to p\bar{p}$, $\Lambda\bar{\Lambda}$, and $B^+ \to p\bar{\Lambda}$ searches, where ϵ is the reconstruction efficiency including the subdecay branching fraction, N_{obs} is the observed number of events in the signal region, N_{exp}^{bg} is the expected background in the signal region, N_{90} is the yield limit at the 90% confidence level, and BF is corresponding upper limit for the branching fraction. The uncertainty in N_{exp}^{bg} is the systematic uncertainty due to the ARGUS parameters and statistical error of the sideband sample.

Mode	ϵ [%]	N_{obs}	N_{exp}^{bg}	N_{90}	BF [10^{-7}]
$B^0 \to p\bar{p}$	17.73	25	26.8 ± 2.3	8.7	<1.1
$B^0 \to \Lambda\bar{\Lambda}$	4.24	3	1.2 ± 0.5	6.1	<3.2
$B^+ \to p\bar{\Lambda}$	8.44	16	12.9 ± 1.7	12.1	<3.2

The expected background contribution is obtained using the sideband region described above. A loose $\mathcal{R}$ requirement is applied to ensure large statistics to determine the ARGUS parameters. The systematic uncertainty in the background prediction comes from the fit errors of the ARGUS parameters and the statistical errors of the events in the sideband region.

The estimated background yields in the signal region are listed in Table III and are close to the number of observed events. Since no statistically significant signals are found, we follow the Feldman-Cousins approach [19] to estimate 90% confidence level (C.L.) upper limits on the signal yields, using the implementation of J. Conrad *et al.* [20] to include the systematic errors. The final results are listed in Table III.

In summary, we have performed a search for the decays $B^0 \to p\bar{p}$, $\Lambda\bar{\Lambda}$, and $B^+ \to p\bar{\Lambda}$ in a sample of 449×10^6 $B\bar{B}$ events, which is 3 times larger than the data set used in the previous analysis [4]. We find no evidence for signals and place 90% C.L. upper limits on the branching fractions of 1.1×10^{-7}, 3.2×10^{-7}, and 3.2×10^{-7} for the $p\bar{p}$, $\Lambda\bar{\Lambda}$, and $p\bar{\Lambda}$ modes, respectively. These upper limits improve our previous results [4] and are more stringent than other experimental limits [5,21]. Moreover, although our $p\bar{p}$ and $p\bar{\Lambda}$ results already reach the pole model predictions [6], no clear signals are seen.

We thank the KEKB group for the excellent operation of the accelerator, the KEK cryogenics group for the efficient operation of the solenoid, and the KEK computer group and the National Institute of Informatics for valuable computing and Super-SINET network support. We acknowledge support from the Ministry of Education, Culture, Sports, Science, and Technology of Japan and the Japan Society for the Promotion of Science; the Australian Research Council and the Australian Department of Education, Science and Training; the National Science Foundation of China and the Knowledge Innovation Program of the Chinese Academy of Sciences under

Contract No. 10575109 and IHEP-U-503; the Department of Science and Technology of India; the BK21 program of the Ministry of Education of Korea, the CHEP SRC program and Basic Research program (Grant No. R01-2005-000-10089-0) of the Korea Science and Engineering Foundation, and the Pure Basic Research Group program of the Korea Research Foundation; the Polish State Committee for Scientific Research; the Ministry of Education and Science of the Russian Federation and the Russian Federal Agency for Atomic Energy; the Slovenian Research Agency; the Swiss National Science Foundation; the National Science Council and the Ministry of Education of Taiwan; and the U.S. Department of Energy.

[1] M.-Z. Wang *et al.* (Belle Collaboration), Phys. Rev. Lett. **90**, 201802 (2003); **92**, 131801 (2004); Y. J. Lee *et al.* (Belle Collaboration) Phys. Rev. Lett. **95**, 061802 (2005).

[2] M.-Z. Wang *et al.* (Belle Collaboration), Phys. Lett. B **617**, 141 (2005).

[3] J. L. Rosner, Phys. Rev. D **68**, 014004 (2003).

[4] M.-C. Chang *et al.* (Belle Collaboration), Phys. Rev. D **71**, 072007 (2005).

[5] B. Aubert *et al.* (*BABAR* Collaboration), Phys. Rev. D **69**, 091503 (2004).

[6] H. Y. Cheng and K. C. Yang, Phys. Rev. D **66**, 014020 (2002).

[7] V. L. Chernyak and I. R. Zhitnitsky, Nucl. Phys. **B345**, 137 (1990); this sum-rule calculation predicts that $\mathcal{B}(B^0 \to p\bar{p}) = 3 \times 10^{-7}$ and the branching fractions of charmless two-body baryonic decays through $b \to s$ penguin transition are $(0.3 \sim 1.0) \times 10^{-5}$.

[8] N. Gabyshev *et al.* (Belle Collaboration), Phys. Rev. Lett. **90**, 121802 (2003).

[9] Charge conjugate modes are implicitly included throughout this paper.

[10] S. Kurokawa and E. Kikutani, Nucl. Instrum. Methods Phys. Res., Sect. A **499**, 1 (2003), and other papers included in this volume.

[11] A. Abashian *et al.* (Belle Collaboration), Nucl. Instrum. Methods Phys. Res., Sect. A **479**, 117 (2002).

[12] Z. Natkaniec *et al.* (Belle SVD2 Group), Nucl. Instrum. Methods Phys. Res., Sect. A **560**, 1 (2006).

[13] R. Brun *et al.*, GEANT 3.21, CERN Report No. DD/EE/84-1, 1987.

[14] E. Farhi, Phys. Rev. Lett. **39**, 1587 (1977).

[15] G. C. Fox and S. Wolfram, Phys. Rev. Lett. **41**, 1581 (1978). The modified moments used in this paper are described in S. H. Lee *et al.* (Belle Collaboration), Phys. Rev. Lett. **91**, 261801 (2003).

[16] R. A. Fisher, Annals of Eugenics **7**, 355 (1937). 1

[17] H. Kakuno *et al.* Nucl. Instrum. Methods Phys. Res., Sect. A **533**, 516 (2004).

[18] H. Albrecht *et al.* (ARGUS Collaboration), Phys. Lett. B **241**, 278 (1990); **254**, 288 (1991).

[19] G. J. Feldman and R. D. Cousins, Phys. Rev. D **57**, 3873 (1998).

[20] J. Conrad, O. Botner, A. Hallgren, and C. Perez de los Heros, Phys. Rev. D **67**, 012002 (2003).

[21] A. Bornheim *et al.* (CLEO Collaboration), Phys. Rev. D **68**, 052002 (2003).